



# **Stable Isotope Profiles Of Skeletal Carbonate Validate Annually-Produced Growth Checks In The Bryozoan *Melicerita chathamensis* From Snares Platform, New Zealand**

By: Marcus M. Key, Jr., Rebecca K. Rossi, Abigail M. Smith,  
**Steven J. Hageman**, & William P. Patterson

## **Abstract**

The bryozoan *Melicerita chathamensis* Uttley and Bullivant, 1972 produces colonies that exhibit visible growth segments defined by narrow growth checks. If these growth checks are annual, then colony age, and seawater variations among seasons and years can be quantified. The purpose of the present study was to use stable isotope profiling to evaluate whether the segments between growth checks represent annual temperature cycles in this species. We applied three independent methods to determine colony age of six colonies from 168 m depth on the Snares Platform located south of New Zealand. First, each colony was X-rayed to determine the location of the growth checks based on skeletal density. Second, branch width was measured for each zooid generation along the growth axis to locate the growth checks. Third, we measured stable C and O isotope values along the colony axis. Branch width patterns corresponded broadly with X-ray patterns, suggesting colony ages of 1.5–7.5 yrs (mean: 4.0 yrs).  $\delta^{18}\text{O}$  profiles suggested colony ages of 4.0–6.5 yrs (mean: 5.3 yrs). This species does precipitate its skeleton in isotopic equilibrium with seawater, such that annual growth checks correlate with cooler winter temperatures. A conceptual model is proposed for the annual growth cycle in this species. In the most complete colony, the  $\delta^{18}\text{O}$ -derived temperatures correlated with inter-annual variations related to the El Niño–Southern Oscillation Index.

Key Jr, Marcus M., Rossi, Rebecca K., Smith, Abigail M., **Hageman, Steven J.**, & Patterson, William P. (2018). Stable isotope profiles of skeletal carbonate validate annually-produced growth checks in the bryozoan *Melicerita chathamensis* from Snares Platform, New Zealand. *Bulletin of Marine Science*, Vol. 94, no. 4, October 2018, pp. 1447-1464. DOI: <https://doi.org/10.5343/bms.2017.1166>. Publisher version of record available at: <http://bullmarsci.org/>



# Stable isotope profiles of skeletal carbonate validate annually-produced growth checks in the bryozoan *Melicerita chathamensis* from Snares Platform, New Zealand

<sup>1</sup> Department of Earth Sciences,  
Dickinson College, P.O. Box 1773,  
Carlisle, Pennsylvania 17013-2896.

<sup>2</sup> Department of Earth Sciences,  
Dartmouth College, 6105  
Fairchild Hall, Hanover, New  
Hampshire 03755.

<sup>3</sup> Department of Marine Science,  
University of Otago, P. O. Box 56,  
Dunedin 9054, New Zealand.

<sup>4</sup> Department of Geology,  
Appalachian State University,  
572 Rivers Street, Boone, North  
Carolina 28608.

<sup>5</sup> Department of Geological  
Sciences, University of  
Saskatchewan, 114 Science Place,  
Saskatoon, SK S7N 5E2, Canada.

\* Corresponding author email:  
<key@dickinson.edu>.

**Marcus M Key Jr**<sup>1\*</sup>  
**Rebecca K Rossi**<sup>2</sup>  
**Abigail M Smith**<sup>3</sup>  
**Steven J Hageman**<sup>4</sup>  
**William P Patterson**<sup>5</sup>

---

**ABSTRACT.**—The bryozoan *Melicerita chathamensis* Uttley and Bullivant, 1972 produces colonies that exhibit visible growth segments defined by narrow growth checks. If these growth checks are annual, then colony age, and seawater variations among seasons and years can be quantified. The purpose of the present study was to use stable isotope profiling to evaluate whether the segments between growth checks represent annual temperature cycles in this species. We applied three independent methods to determine colony age of six colonies from 168 m depth on the Snares Platform located south of New Zealand. First, each colony was X-rayed to determine the location of the growth checks based on skeletal density. Second, branch width was measured for each zooid generation along the growth axis to locate the growth checks. Third, we measured stable C and O isotope values along the colony axis. Branch width patterns corresponded broadly with X-ray patterns, suggesting colony ages of 1.5–7.5 yrs (mean: 4.0 yrs).  $\delta^{18}\text{O}$  profiles suggested colony ages of 4.0–6.5 yrs (mean: 5.3 yrs). This species does precipitate its skeleton in isotopic equilibrium with seawater, such that annual growth checks correlate with cooler winter temperatures. A conceptual model is proposed for the annual growth cycle in this species. In the most complete colony, the  $\delta^{18}\text{O}$ -derived temperatures correlated with inter-annual variations related to the El Niño–Southern Oscillation Index.

---

**Section Editor:** Aaron O’Dea

Date Submitted: 7 November, 2017.  
Date Accepted: 4 April, 2018.  
Available Online: 4 April, 2018.

Marine skeletal carbonate can be a useful and persistent biogeochemical proxy of seawater conditions, especially temperature, but such proxies are only useful when well calibrated temporally. In taxa like the bryozoans, where growth rate is poorly known and can vary greatly (Smith 2014), one approach—used in polar faunas—has been to rely on growth checks. Growth checks are areas of thickened skeleton that are thought to indicate slow-to-no growth during food-scarce Antarctic winter (Brey et al. 1999, Smith 2007). However, there has not been a study that validates the

annual nature of similar growth checks in temperate bryozoans using stable isotope-derived temperatures, where the signal more likely approximates temperature rather than food availability.

Previous studies on temperate bryozoans have used three different approaches to calibrate growth checks to annual sea water temperature cycles. These have included repeated sampling over the course of a year to document growth cessation, using zooid size as a proxy for temperature, and finally using oxygen isotope values as a proxy for temperatures. Stebbing (1971) began by correlating skeletal growth check lines in *Flustra foliacea* (Linnaeus, 1758) to annual seasons using repeated monthly sampling. Pätzold et al. (1987) correlated less calcified growth bands in *Pentapora foliacea* (Ellis and Solander, 1786) to winter using oxygen isotope profiles. Most recently, Lombardi et al. (2008) used X-rays to define growth checks in *Pentapora* sp.

These early approaches worked only with species that have visible growth checks. The zooid size approach does not require this. It is based on the empirical observation that an inverse relationship exists between zooid size and temperature (O'Dea and Okamura 2000). Based on this temperature-size relationship, O'Dea and Okamura (2000) developed a model relating intra-colony zooid size variation to the mean annual range in temperature. Since then, this mean annual range of temperature (or, MART) technique has been applied to modern and ancient environments (O'Dea and Jackson 2002, O'Dea 2003, 2005, Lombardi et al. 2006, Knowles et al. 2009, McClelland et al. 2014).

The latest approach uses oxygen isotope values as a proxy for temperature. Stable C and O isotope values derived from bryozoan skeletal carbonate have been used to address growth and carbonate production rates (Pätzold et al. 1987, Brey et al. 1999, Bader 2000, Smith and Key 2004, Bader and Schäfer 2005), physiological and ecological effects of symbionts and food sources (Crowley and Taylor 2000, Key et al. 2005a, van Hardenbroek et al. 2016), and diagenetic recrystallization and cementation (Key et al. 2005b). Stable isotopes have also been effective in documenting temporal changes in temperature in bryozoan carbonate (Pätzold et al. 1987, Smith and Key 2004, Knowles et al. 2010, Key et al. 2013a,b), and are thus an appropriate tool for examining the relationship between temperature and growth checks, as well as inter-annual variability in growth rate.

The innovative aspect of the present study is the combination of these three approaches: growth check-lines (determined from X-rays), zooid size (or branch size), and isotopes profiles for determining species growth. Our aim was to reconstruct annual seawater temperature profiles using stable isotope profiles in the extant temperate bryozoan *Melicerita chathamensis* Uttley and Bullivant, 1972 from the Snares Platform south of New Zealand, thus developing a conceptual growth model in this species. Growth cycles can be correlated with morphologic growth segments defined by independently-identified growth checks to calculate mean annual ranges in temperature, colonial growth rates, and to compare the bryozoan-carbonate temperature record to known annual and inter-annual variations in seawater temperature.

## MATERIALS AND METHODS

**STUDY SITE AND SAMPLE COLLECTION.**—The study site (Fig. 1) is located near the Sub-Tropical Front (STF), a Southern Hemisphere, dynamic thermohaline oceanic water mass boundary sometimes referred to as the Sub-Tropical Convergence.

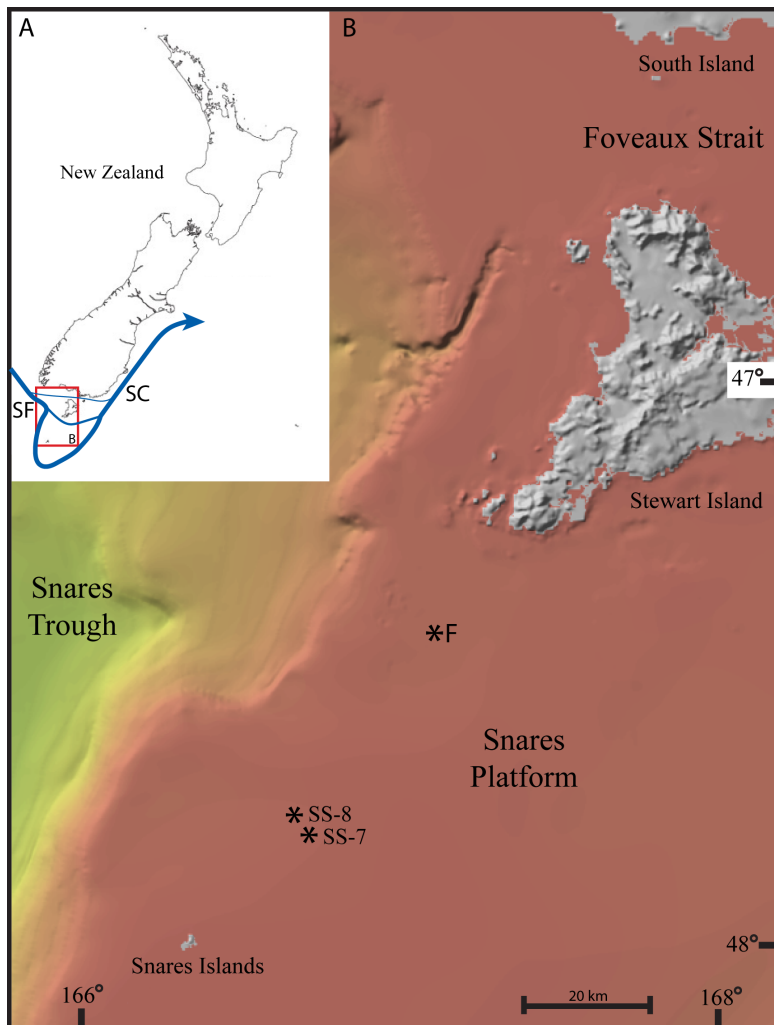


Figure 1. Topographic and bathymetric map of the Snares Platform, New Zealand showing study sites (\*) relative to closest time series CTD data from Chiswell's (1996) West Snares Mooring F (F). The local expression of the subtropical front, the Southland Front (SF), is noted in the smaller map with the line width proportional to the relative flows which merge to form the Southland current (SC). (Modified from NIWA's 250 m gridded bathymetric data set: <http://www.niwa.co.nz/our-science/oceans/bathymetry>.)

The STF separates the warmer, more saline, nutrient-poor Sub-Tropical Water to the north from the colder, less saline, nutrient-rich sub-Antarctic water to the south (Sikes et al. 2002, Hopkins et al. 2010). Rather than a single well-defined front, others describe the STF as a zone between a North-STF and a South-STF with multiple branches. Part of the South-STF passes through Foveaux Strait, more of it flowing across the Snares Platform, but the majority of it wraps around the edge of the shelf break of the Snares Platform and through the Snares Depression south of our site before diverting sharply northward along the southeast coast of the South Island, where it becomes the single well-defined, narrow Southland Current (Hopkins et al. 2010, Smith et al. 2013). The STF is locally known as the Southland Front (SF) (Fig.

1A). The SF migrates latitudinally with the seasons (Hopkins et al. 2010, Campanelli et al. 2011), but around the Snares Platform it migrates little due to bathymetric steering (Shaw and Vennell 2001). Regionally, the mixed surface layer near the STF shows more seasonal variation in temperature than salinity (Rintoul et al. 1997). There is a 1-to-2-mo delay between the seasonal temperature extremes around New Zealand at the surface and at 100 m depth due to vertical mixing (Garner 1969). The closest time series (i.e.,  $\geq 1$  yr record) data to our study site comes from Chiswell's (1996) West Snares Mooring F, 45 km to the northeast and at 80 m depth (see Fig. 1B), which measured a mean annual range in temperature of 4.0 °C (i.e., 10.4–14.4 °C, mean: 11.8 °C).

Sampling of the bryozoan *M. chathamensis* was carried out from the University of Otago's research vessel, RV POLARIS II, during the austral summer in December 2011. The benthic fauna was sampled by bottom box dredge (60 cm  $\times$  26 cm with a 5 mm wire mesh) at station SS-7 (47.85087°S, 166.71227°E) at a depth of 168 m (Fig. 1B). Living colonies of *M. chathamensis* were picked out of the dredge material immediately after collection.

*Melicerita chathamensis* is a cheilostome bryozoans, which means its individual zooid animals secrete box-like ( $< 1$  mm<sup>3</sup>) carbonate skeletons that are connected into a blade-like colony. The growth axis of the blade is oriented parallel to the long axis of the branch and roughly perpendicular to the substratum. This species lives as an erect blade attached to the sea floor by rootlets and forms colonies of scimitar-shaped, bilaminar, unbranched blades. The branches exhibit subtle growth segments defined by narrow growth checks or constrictions (Uttley and Bullivant 1972, Smith and Lawton 2010) (Fig. 2).

We collected 14 fresh, unbroken colonies and selected the six largest (labelled MC1–4, 7–8). Broken and repaired or regenerated colonies were avoided. Due to drift, we measured water temperature and salinity at a second station, SS-8 (47.84185°S, 166.72028°E), that was 1.168 km from SS-7 and at a water depth of 161 m (Fig. 1B). Sites SS-7 and SS-8 are similar in depth (7 m, Fig. 1), and probably also in salinity and temperature (see below) as the water is well mixed here (Smith et al. 2013, fig. 9). At SS-8 we carried out a two-way vertical conductivity-temperature-depth (CTD) cast. Salinity was measured to the nearest 0.0001, temperature to the nearest 0.0001 °C, and depth to the nearest 0.001 m. A bottom water sample was collected and fixed on board with mercuric chloride and was sent for carbon and oxygen isotope analysis.

**X-RAY AND MORPHOMETRIC ANALYSIS OF GROWTH CHECKS.**—To avoid any possible effects of pretreatment on carbonate skeletal isotope values (Forester et al. 1973; M Key, Dickinson College, unpubl data), we did not use bleach or hydrogen peroxide to remove the organic components of the colonies analyzed for isotope analysis. The colonies were dried, measured, weighed, and X-rayed (Fig. 3A) with a Toshiba (Japan) floor-mounted X-ray unit housing a Molybdenum X-ray tube, using Industrex M-film, and settings of film-focus distance = 60 cm, 200 Ma, 32 kVp, 0.16 s. Each colony was digitally photographed under reflected light. Scanning electron microscope (SEM) imaging of one colony not used in the analysis (i.e., Fig. 2) required removal of the cuticle by light bleaching. The SEM was a JEOL 6700F field emission SEM (JEOL Ltd, Tokyo, Japan) fitted with a JEOL 2300F EDS system (JEOL Ltd, Tokyo, Japan) and a Gatan Alto 2500 cryo preparation chamber/cryo stage (Gatan Inc, Pleasanton, California). Adjacent overlapping SEM images were stitched together using Adobe Photoshop's automated Photomerge™ feature.

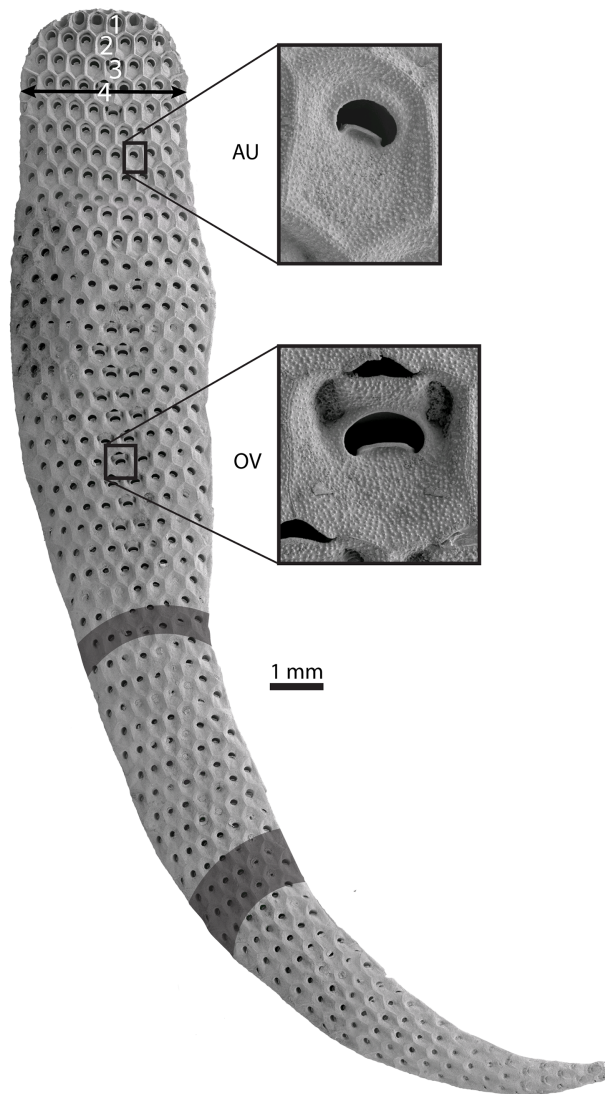


Figure 2. Composite scanning electron microscope (SEM) image of *Melicerita chathamensis* colony MC10 showing numbering of zooid generations (1–4) from the growing tip, measurement of branch width at zooid generation four, examples of a regular feeding autozooid (AU) and an autozooid with ovicell for larval brooding (OV), and examples of a range of micromilling paths (gray bands). Zooid generations refer to the rows of zooids (numbered 1–4) from the growing tip with 1 being the most recently formed, 2, the previous generation, etc. This colony was not used in our analysis as the organic matter was removed by bleaching for SEM imaging.

Individual zooid generations making up the colony were counted in each specimen from the growing tip to the colony base along the growth axis (*see e.g.*, Fig. 2). Colony length was measured along the colony growth axis to the nearest 0.1 mm. Branch width was measured at the midpoint of the zooid along the colony axis (Fig. 2) to the nearest 0.01 mm, orthogonal to the colony growth axis for each zooid generation. Branch width is a function of both the number of zooids across the branch as well as the size of individual zooids.



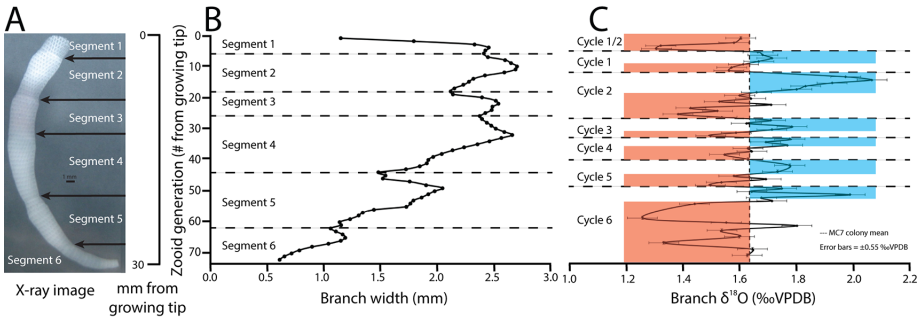


Figure 3. Correlation of results from (A) X-ray, (B) branch width, and (C)  $\delta^{18}\text{O}$  methods for defining growth segments and annual  $\delta^{18}\text{O}$ -derived temperature cycles for *Melicerita chathamensis* colony MC7. Red (left shading in C) = warmer months, blue (right shading in C) = colder.

Variation in brightness in the X-ray images due to fluctuations in skeletal density were used to define growth segments (Fig. 3A). Growth segments between checks in each colony were counted independently by the first four authors to cross-validate X-ray images and branch-width profiles using the following methods. Based on slightly different results, sometimes for the same colony among the authors, this was the most subjective of the three methods. Growth segments were also counted using the branch-width measurements to discern constrictions along the colony edges (Fig. 3B) mentioned by Uttley and Bullivant (1972) in their original description of their new species. As with zooid generations, growth segments were numbered from the growing tip down to the colony base.

We inferred colony age from growth segment counts (Fig. 3A–B) by counting the partial segment at the growing tip as a half year and all the other segments as a full year. We assumed that the larvae of this species settle in the spring like most cold-water New Zealand bryozoans (Gordon and Mawatari 1992). Therefore, the basal growth segment represents spring to winter. The next growth segment incorporates the following year's spring to winter growth, and the last growth segment formed from spring to the collection date, which was in midsummer. So in a three-segment colony, the basal segment represents a full year, the middle segment, another full year, the last segment a half of a year, resulting in a colony age of 2.5 yrs.

**MICROMILLING AND STABLE ISOTOPE MASS SPECTOMETRY.**—Powder aliquots for stable isotope analysis were micromilled (*sensu* Wurster et al. 1999) with New Wave Research's Merchantek MicroMill™ automated microsampler using a 0.5 mm Brassler carbide dental drill bit. Micromilling paths were made for each generation of zooids along the length of the branch oriented parallel to the branch's arcuate growing tip (Fig. 2). Thus, a time-series profile was serially created from the base of the colony (i.e., the oldest part where the founding larva metamorphosed into the first zooid, the ancestrula) toward the top of the colony (i.e., the youngest part) along the growth axis. Entire zooids in each generation were micromilled. Due to budget limitations, the four smaller colonies (MC1–4) were sampled with a coarser resolution (i.e., 6–13 samples from the 24–62 total zooid generations per colony = 23% of zooid generations micromilled) than the two largest colonies (MC7–8: 58–61 samples from the 70–72 total zooid generations per colony = 84% of zooid generations). Powder from the pulverized carbonate skeleton was collected with a scalpel

at the end of each pass. Between passes, any remaining powder was removed from the colony, drill, and stage with compressed air. Collected powder was placed in a stainless steel boat, which was weighed before and after filling to ensure sufficient carbonate (i.e.,  $\geq 20 \mu\text{g}$ ). Boats were placed in brass convoys and sealed with a Teflon gasket for shipment.  $\delta^{18}\text{O}$  and  $\delta^{13}\text{C}$  isotope analyses were performed at the University of Saskatchewan Isotope Laboratory, Saskatoon, Canada.

Carbonate samples were roasted in vacuo at  $200^\circ\text{C}$  for 1 hr to remove water and volatile organic contaminants that may confound stable isotope values of carbonates. Stable isotope values were obtained using a Finnigan<sup>TM</sup> Kiel-IV carbonate preparation device directly coupled to the dual inlet of a Finnigan<sup>TM</sup> MAT 253 isotope ratio mass spectrometer. A range of  $20\text{--}50 \mu\text{g}$  of carbonate was reacted at  $70^\circ\text{C}$  with 3 drops of anhydrous phosphoric acid for 420 s. The  $\text{CO}_2$  evolved was then cryogenically purified before being passed to the mass spectrometer for analysis. Isotope ratios were corrected for acid fractionation and  $^{17}\text{O}$  contribution using the Craig (1957) correction. Isotope ratios are reported in per mil notation (‰) relative to the IAEA Vienna Pee Dee Belemnite (VPDB) scale using the standard  $\delta$  notation where:  $\delta_{\text{sample}} = ((R_{\text{sample}}/R_{\text{standard}}) - 1) \times 10^3$ . R is the  $^{18}\text{O}/^{16}\text{O}$  or  $^{13}\text{C}/^{12}\text{C}$  ratio.

Using the standard Kim et al. (2007) correction,  $\delta^{18}\text{O}_{\text{carb}}$  values reflect the aragonite-calcite difference in isotopic fractionation during acidification. Data were directly calibrated against Friedman et al.'s (1982) NBS-19 standard that is by definition  $\delta^{18}\text{O}_{\text{carb}} = -2.2\text{‰}$  VPDB and  $\delta^{13}\text{C}_{\text{carb}} = 1.95\text{‰}$  VPDB. Precision/accuracy of data was monitored through routine analysis of NBS-19 and in-house check standards that have been stringently calibrated against NBS-19. The precision of  $\delta^{18}\text{O}_{\text{carb}}$  and  $\delta^{13}\text{C}_{\text{carb}}$  are  $0.11\text{‰}$  VPDB and  $0.05\text{‰}$  VPDB, respectively.

Of the 161 paths micromilled, 160 were successfully collected, and 159 successfully analyzed. Of the 159 samples, one had too little powder to generate the minimum signal intensity of 100 mV to return an accurate value from the mass spectrometer. Two samples had too little powder to generate the minimum signal intensity of 450 mV to return a dependable value from the mass spectrometer, so these failures were also removed, yielding a total of 157 samples. Lost samples are a function of the methodological challenge of balancing the need for obtaining enough carbonate powder to get a reliable result from the mass spectrometer (i.e.,  $>20 \mu\text{g}$ ) and minimizing the width of each micromill path so as to minimize time averaging by not including multiple zooid generations.

*Melicerita chathamensis* precipitates a calcite skeleton (Smith and Lawton 2010). Thus, we used our measured  $\delta^{18}\text{O}_{\text{sw}}$  of  $+0.7\text{‰}$  VSMOW and corrected for conventional  $\text{CO}_2$ -calcite acid fractionation factor of 1.01025 in Kim and O'Neil's (1997) calcite paleotemperature equation to calculate water temperature from each of our 157 samples.

Finally, we used Key et al.'s (2013b) methodology of determining annual growth cycles from the  $\delta^{18}\text{O}$  profile (e.g., Fig. 3C) relative to the mean value for the colony. An annual cycle is defined by three consecutive crossings of the colony mean. Each crossing is preceded and followed by two or more consecutive data points on opposite sides of the mean (akin to a vertical sine wave crossing its mean). The three consecutive crossings represent one annual cycle of warmer and colder temperatures. As with zooid generations and growth segments, isotope cycles were numbered from the growing tip down to the colony base.



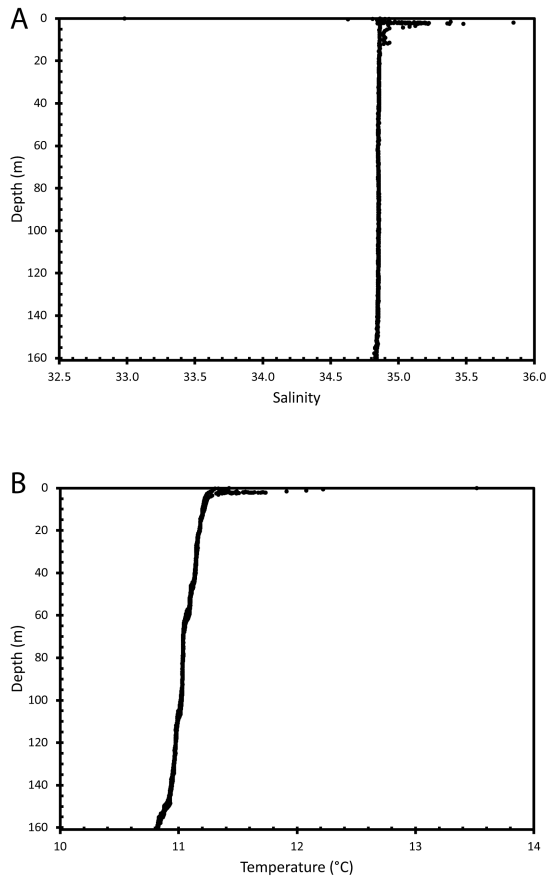


Figure 4. Salinity (A) and temperature (B) depth profiles from station SS-8 on 7 December, 2011.

## RESULTS

The near-vertical CTD profiles taken at the study site (Fig. 4) indicate that the water is well-mixed. On the Snares Platform, there is strong tidal action and wind-forced mixing of the entire water column (Butler et al. 1992). Across the profile, salinity shows a mean of 34.88 (Fig. 4A, range: 32.98–35.85, SD 0.12). On the seafloor 1.168 km from where the bryozoans were living, it was 34.83 at the time of collection. Average temperature was 11.1 °C (Fig. 4B, range: 10.8–13.5, SD 0.2 °C). On the seafloor where the bryozoans were living, it was 10.8 °C at the time of collection. The bottom water sample had stable isotope values of 0.7‰ VSMOW for  $\delta^{18}\text{O}_{\text{sw}}$  and 1.2‰ VPDB for  $\delta^{13}\text{C}_{\text{sw}}$ . Due to logistical constraints of only being able to stay on station for a few hours, no data were collected on the seasonal variation in temperatures on the sea floor at the collecting locality. The closest available time series (i.e.,  $\geq 1$  yr record) data to our study site comes from Chiswell's (1996) West Snares Mooring F, 45 km to the northeast and at 80 m depth (see Fig. 1B).

Colonies ranged in length from 9.3 to 29.5 mm (Table 1). The number of zooid generations per colony varied proportionally with colony size and ranged from 24

Table 1. Colony size and isotope sampling density of the six bryozoan colonies belonging to *Melicerita chathamensis*.

Colony ID	Length (mm)	Zooid generations	Micromill paths	Zooid generations micromilled (%)
MC1	9.3	24	7	29
MC2	10.3	28	6	21
MC3	23.5	62	13	21
MC4	23.2	56	12	21
MC7	27.7	72	58	81
MC8	29.5	70	61	87
Summary statistics				
Minimum	9.3	24	6	21
Mean	20.6	52	26	43
Maximum	29.5	72	61	87
Standard deviation	7.9	19	24	29

to 72. The ages of the colonies inferred from the number of growth segments varied proportionally with colony size (Table 2). The X-ray images yielded a mean age for the six colonies of 4.5 yrs ( $n = 6$ , range: 1.5–7.5, SD 2.0 yrs). The branch width method yielded a mean of 3.5 yrs ( $n = 6$ , range: 1.5–6.5, SD 1.9 yrs).

In total, 157 successful paths (161 attempted) were micromilled across the six colonies. The number of paths per colony varied proportionally with colony size (Table 1). Path widths ranged from 1 to 3 zooid generations (mean: 1.2, SD 0.4); 85% of our samples included one zooid generation, 15% two, <1% three. The micromill paths generally included more zooid generations at the colony base because the branches widened toward the top (Fig. 2), and at least 20  $\mu\text{g}$  of carbonate was needed for the mass spectrometer. As a result, the temporal resolution of the isotope sampling increased upward through each colony.

Table 2. Estimate of colony ages and growth rates from growth checks inferred from X-rays, growth checks inferred from branch widths, and annual  $\delta^{18}\text{O}$  cycles. Asterisk indicates too coarsely sampled to determine colony age.

Colony ID	MC1	MC2	MC3	MC4	MC7	MC8	Mean (SD)	Mean number of zooid generations per year
Length (mm)	9.3	10.3	23.5	23.2	27.7	29.5	20.6 (7.9)	
Age (yr) from X-rays	2.5	1.5	5.5	4.5	5.5	7.5	4.5 (2.0)	11.3
Age (yr) from branch widths	1.5	1.5	3.5	2.5	5.5	6.5	3.5 (1.9)	11.6
Age (yr) from $\delta^{18}\text{O}$ cycles	*	*	*	*	6.5	4.0	5.3 (1.3)	13.5
Mean age (yr) ( $n = 2$ or 3)	2.0	1.5	4.5	3.5	5.8	6.0	3.9 (1.7)	12.1
Age coefficient of variation (%)	25.0	0.0	22.0	29.0	8.0	25.0	18.0 (11.0)	
Mean growth rate (mm yr <sup>-1</sup> )	4.7	6.9	5.2	6.6	4.7	4.9	5.5 (0.9)	

$\delta^{18}\text{O}$  values from all the colonies ranged from 1.1‰ to 2.4‰ VPDB (mean: 1.7‰, SD 0.2‰ VPDB).  $\delta^{13}\text{C}$  values from all the colonies ranged from 1.1‰ to 2.6‰ VPDB (mean: 1.7‰, SD 0.3‰ VPDB). To determine if the  $\delta^{18}\text{O}$  values were skewed by any vital effects (*sensu* Erez 1978), we compared the water temperatures measured on the seafloor (1.168 km away at station SS-8) with those calculated from the  $\delta^{18}\text{O}$  values derived from the growing tips of the colonies at station SS-7. We attempted to sample just the actively developing zooids at the growing tip. In half of the six colonies, due to the coarseness of sampling, we incorporated some of the second generations' previously formed zooids. Depending on the colony growth rate, these second generation zooids may have formed under different water conditions. Based on Chiswell's (1996) time series data from the West Snares Mooring F, any difference was probably minimal, and potentially only affected half of the colonies.

According to Smith and Lawton (2010), this species incorporates Mg into skeletal calcite at values ranging from 0.8 to 9.7 wt%  $\text{MgCO}_3$  (mean: 4.1 wt%  $\text{MgCO}_3$ ). Low-Mg calcite (mean: 2.1 wt%  $\text{MgCO}_3 = 1.7 \text{ mol}\% \text{MgCO}_3$ ) dominates at the growing tip, and high-Mg calcite is gradually added with age. Due to the presence of Mg, we used the standard Tarutani et al. (1969)  $\delta^{18}\text{O}_{\text{calcite}}$  correction for Mg. These corrected calculated water temperatures from the six colony growing tips averaged 10.8°C (range: 10.4–11.5, SD 0.4 °C), exactly the same as the water temperatures measured on the seafloor. In addition, skeletal carbonates influenced by a vital effect can exhibit a positive correlation between  $\delta^{13}\text{C}$  and  $\delta^{18}\text{O}$  values (Keith and Weber 1965, Erez 1978, Romanek and Grossman 1989). Such covariation can also indicate a relationship between metabolism, reproduction, or food supply and temperature (Patterson 2017). Regardless, no significant correlation ( $R^2 = 0.070$ ,  $P > 0.05$ ) was observed suggesting no vital effect on the  $\delta^{18}\text{O}$  values in this species.

$\delta^{13}\text{C}$  values pooled among colonies are significantly and positively correlated with branch width (linear regression:  $R^2 = 0.092$ ,  $P < 0.001$ ) and increase significantly from colony base to growing tip (linear regression:  $R^2 = 0.259$ ,  $P < 0.001$ ). In contrast, there are no significant patterns in  $\delta^{18}\text{O}$  values with zooid generation number or branch width (linear regressions:  $P > 0.05$ ). Looking at each colony individually,  $\delta^{13}\text{C}$  values show no apparent pattern, but  $\delta^{18}\text{O}$  values show a distinct zig-zag pattern up through the colony (e.g., colony MC7 in Fig. 3C), which is discussed below.

The isotope profiles yielded an average age of 5.3 yrs ( $n = 2$ , range: 4.0–6.5, SD 1.3 yrs). The slightly higher ages from the isotope profiles is partly an artifact of excluding the more coarsely sampled smaller/younger colonies (MC1–4). To illustrate the results of the different methods, we chose the colony MC7 as it is one of the largest and most densely sampled colonies and has the most zooid generations (Table 1). Additionally other than the little colony MC2, colony MC7 has the lowest coefficient of variation (i.e., 8%) in inferred ages (Table 2) indicating the three methods for determining age are very consistent in this colony. In colony MC7, the X-ray image and branch width profile show six segments (i.e., 5.5 yrs of growth), while the isotope profile shows 6.5 annual cycles (Fig. 3A–C). Colony MC8 produced less clear results with 7.5 yrs of growth indicated by the X-rays, but only 4.0 annual isotope cycles. These intracolony differences are attributed to the different methodologies. Despite this, the two largest and most completely analyzed colonies (MC7–8) yield similar mean ages (6 yrs) from the three methods.

Using only complete segments or complete isotope cycles (i.e., excluding the topmost segments/cycles at the growing tips) in the largest and most completely

analyzed colonies (MC7–8), the number of zooid generations per year for all three methods combined averaged 12.1 (range: 5–22, SD 1.0, Table 2).

We then compared two subsamples of isotope values, the first consisting of  $\delta^{18}\text{O}$  values from growth checks, (i.e., the narrowest parts of the branch in each segment); the second subsample consisting of values from the widest parts of the branch in each segment. Values were pooled across colonies without regard for growth position and were unpaired between individual growth check vs widest parts. For each subsample,  $n$  = total number of segments summed across all colonies (Fig. 3). There was a significant difference between the mean  $\delta^{18}\text{O}$  values of the two subsamples; growth checks = 1.8‰ VPDB and the widest parts of branch segments = 1.6‰ VPDB (two sample  $t$ -test:  $df = 28$ ,  $t = 2.258$ ,  $P = 0.032$ ), indicating that on average, growth checks formed in colder water than the widest parts of the branches. The calculated mean  $\delta^{18}\text{O}$ -based water temperature was 11.6 °C (range: 8.4–14.0, SD 1.0 °C). The  $\delta^{18}\text{O}$ -based mean annual range in temperature in the largest and most completely analyzed colonies (MC7–8) averaged 2.5 °C ( $n = 10$  isotope cycles, range: 0.7–4.7, SD 1.4 °C). In contrast, there was no significant difference between the mean  $\delta^{13}\text{C}$  values of the growth checks and the widest part of the branch in each segment (two sample  $t$ -test:  $P = 0.608$ ).

## DISCUSSION

**ANNUAL GROWTH CHECKS AND TEMPERATURE PROFILES.**—Based on the general correlation between the number of growth segments and water temperature-induced isotope cycles, we interpret growth segments in *M. chathamensis* as annual records. We envision a conceptual model for the development of annual growth segments in this species driven by seasonal temperature cycles (Jillett 1969, Chiswell 1996) and the resulting changes in food availability (Murphy et al. 2001) for the bryozoans.

As indicated in Table 3, each growth segment begins at the current growth edge (though this is the proximal end of the segment once it is formed) with the annual “growth check” of Stebbing (1971), the “constriction” of Uttley and Bullivant (1972), or the “node” of Brey et al. (1998). The growth checks form in the winter when temperatures are coldest, food least available, and growth slowest. This creates the darkest part of the X-ray image, meaning calcification is densest due to slow or no linear growth combined with continued calcification to thicken the skeleton. Previous studies attributed the growth checks to cold water (Pätzold et al. 1987, Bader and Schäfer 2004, Smith and Key 2004, Smith 2007), and we confirm that here. The arrival of warmer spring temperatures initiates the first plankton bloom, and the colony starts to grow faster and wider. Peak temperatures and decreased food supply occur during summer. Late summer into early autumn marks the widest part of the segment, often due to the growth of reproductive ovicells that are wider than the regular feeding autozooids (Uttley and Bullivant 1972, fig. 16) (Fig. 2). The general widening of the colony upward is accomplished by adding another complete zooid at the growing tip every few zooid generations. The subtle widening of the branch as part of a growth segment is due to widening of existing zooids due to the growth of ovicells. Late autumn to early winter brings decreasing water temperatures and less food as growth slows and the branch narrows. Using only our most completely sampled colony (MC7), the mean number of zooid generations grown during the summer is 41% higher than that in the winter (i.e., 6.4 vs 4.5). This conceptual model explains why

the annual  $\delta^{18}\text{O}$  cycles are offset from the growth segments defined by the growth checks. The growth segments are not only controlled by water temperature, but also food availability, and the two are not in sync (Table 3).

We do not observe a concomitant change in  $\delta^{13}\text{C}$  values in response to the seasonal changes in food (Murphy et al. 2001) and growth rate. That signal, if present, may be overwhelmed by the colony-level signal of increasing  $\delta^{13}\text{C}$  values from the colony base to the growing tip. Why are the  $\delta^{13}\text{C}$  values increasing as the colony grows and develops? It may be due to changes in the isotope value of dissolved inorganic carbon, which the bryozoan is extracting from the water or from changing skeletal carbonate mineralogy. Alternatively, it may be due to the taller colonies having access to plankton with different isotopic composition as they extend up into the water column.

Bader and Schäfer (2005) attributed some changes in  $\delta^{13}\text{C}$  values in bryozoan skeletons to seasonal variation in the input of organic rich matter, especially from resuspension of organic matter on the sea floor, which has slightly higher  $\delta^{13}\text{C}$  values compared to fresh food. Our  $\delta^{13}\text{C}$  data do not show fluctuations like this, but we cannot rule it out as we did not measure  $\delta^{13}\text{C}_{\text{sw}}$  over time. Alternatively, the increasing  $\delta^{13}\text{C}$  values through colony development (i.e., astogeny) could be due to decreasing wt%MgCO<sub>3</sub> from the base to the growing tip (Smith and Lawton 2010). The presence of Mg in calcite has been shown to affect  $\delta^{13}\text{C}$  values (Tarutani et al. 1969, Jimenez-Lopez et al. 2006; M Key, Dickinson College, unpubl data).

In bryozoans, the number of zooid generations per year varies in response to environmental, astogenetic, and colony factors. Environmental factors include inter-annual differences in food availability and temperature (O'Dea and Okamura 1999). Astogenetic factors include metabolic rate changing over the course of the colony's history (Bader and Schäfer 2005). Colony factors include micro-environmental and genetic differences among colonies (Hageman et al. 1999).

If the number of zooid generations varies annually, what is the best method for aging colonies? The X-ray method provides the highest resolution and easiest method for counting growth segments, but it is the most subjective. Branch width is more objective, but it can be partially compromised by branch swelling from ovicell growth. The isotope method is the most expensive, most time consuming, and least spatially resolvable method, but the only method that directly correlates the growth segments with seasonal temperature cycles. Despite the robustness of three independent methods for aging colonies in the present study, our sample size is not sufficient to statistically discriminate between the relative effects of environmental, astogenetic, and colony factors on the number of zooid generations per year.

We can, however, calculate colony growth rates by dividing colony length by mean colony age (Table 2). Growth rates ranged from 4.7 to 6.9 mm yr<sup>-1</sup> (mean: 5.5, SD 0.9 mm yr<sup>-1</sup>). These values fall within the range of other bryozoan species from a variety of environments using a variety of methodologies (Smith 2014). Smith and Lawton (2010) calculated growth rates in the same species from the same locality but different years and found a similar mean rate of 5.3 mm yr<sup>-1</sup> ( $n = 41$ , range: 1.3–13.7 mm yr<sup>-1</sup>).

The  $\delta^{18}\text{O}$ -based mean annual range in temperature in the largest and most completely analyzed colonies (MC7–8) averaged 2.5 °C. The closest time series (i.e.,  $\geq 1$  yr record) data to our study site comes from Chiswell's (1996) West Snares Mooring F, 45 km to the northeast and at 80 m depth (see Fig. 1B), which measured a mean annual range in temperature of 4.0 °C (i.e., 14.4–10.4, mean: 11.8 °C). This range is

1.5 °C more than ours (i.e., 4.0–2.5 °C), which could be due to the 81 m (i.e., 161–80 m) depth difference. Seasonal variation in water temperature around New Zealand decreases with depth due to convective overturn from 6–8 °C at the surface to approximately 2 °C at 150 m, with little seasonal variation below 200 m (Jillett 1969, Ridgway 1969, Heath 1985, Rahmstorf 1992). Our mean annual range in temperature is also similar to Jillett's (1969, table 1) from the Southland Current (i.e., a northeast extension of the SF) at 3.5 °C (i.e., 12.0–9.5 °C). Our study site is also located in the Southland Current, but well upstream (360 km southwest) of Jillett's (1969) study site.

The seasonal water temperature cycle is partly responsible for the seasonal phytoplankton blooms, which ultimately provide food to the benthic filter-feeding bryozoans, affecting growth rate. Murphy et al. (2001) mapped the seasonal variation in chlorophyll *a* around New Zealand. They documented a distinctly bimodal plankton bloom in the STF region west of the South Island whose currents flow across the Snares Platform. The bimodal distribution begins with a first bloom in the spring (i.e., October–November), followed by a brief decline in the middle of summer (i.e., January), and a second bloom in late summer–early autumn (i.e., March–April). Food availability affects colony growth rate and thus the development of the growth segments (Table 3).

**INTER-ANNUAL TEMPERATURE VARIATIONS.**—Bryozoan colonies grow by accretion, reaching up to 2 m in size (Cocito et al. 2004, Lombardi et al. 2010) and can live for >100 yrs (Reid 2014, Smith 2014). In general, bryozoans precipitate their skeletal CaCO<sub>3</sub> in isotopic equilibrium with sea water (*see* review in Key et al. 2005a). The effects of food sources and water temperature on stable C and O isotope values have been well documented (Brey et al. 1999, Bader and Schäfer 2005, O'Dea 2005, Key et al. 2013a,b). Due to the genetically identical, asexually replicated zooids in a colony, stable C and O isotope profiles obtained from skeletons of long-lived colonies are ideal for quantifying environmental change.

To quantify longer term (i.e., inter-annual) maximum temperature variation, we averaged the 10 coldest and 10 warmest water temperatures derived from the δ<sup>18</sup>O values from all the colonies. Based on inferred mean colony ages (Table 2), this represents a 6 yrs maximum range of 4.0 °C (i.e., 13.4–9.4 °C). This order of multi-year temperature variation is probably caused by inter-annual variations in the El Niño–Southern Oscillation Index (SOI) (Ashcroft et al. 2016). To test this notion in our most completely sampled colony (MC7), we compared our data to the difference between the mean summer and winter SOI values from the National Oceanic and Atmospheric Administration (NOAA, <https://www.ncdc.noaa.gov/teleconnections/enso/indicators/soi/data.csv>).

We used NOAA's monthly data from 2005 to 2011 (based on a colony collection date of December 2011 at the colony tip). Counting back toward the colony base using the isotope cycles from Figure 3C and the inferred years from Table 2, we correlated SOI monthly values to isotopic summers and winters. There were no significant correlations between the summer, winter, or annual SOI and the isotope-derived water temperatures in colony MC7. The difference between mean winter and summer isotope-derived water temperatures in colony MC7 were significantly inversely correlated with the difference between mean winter and summer SOI values from 2005 to 2011 (linear regression:  $R^2 = 0.717$ ,  $P = 0.033$ ). This means that as the SOI



varies seasonally from year to year, seasonal temperature differences recorded in the  $\delta^{18}\text{O}$  values from bryozoan skeletal carbonate on the Snares Platform are responding, but inversely. ENSO-driven changes in the position of the Southern Hemisphere's STF relative to the Snares Platform (Tilburg et al. 2002, Hopkins et al. 2010) may produce this effect, or it may be due to an ocean circulation-driven lag time. Belkin and Cornillon (2003) showed that the position of the STF south of New Zealand varies year-to-year. At times, it may pass around or directly cross the Snares Platform, with the STF occasionally splitting into multiple branches upstream (Fig. 1A), which may exist simultaneously in the across shelf and around shelf positions.

This discussion of inter-annual temperature variations is based on only the longest, most densely sampled colony. Obviously a sample size of one cannot provide definitive results. The difficulty of acquiring samples of this kind, combined with finite resources, limits sample size. We include this discussion on the basis that it provides more data than ever before, and provides guidance to future research on the topic.

This approach can also be applied to paleoclimate studies using fossils, but with the following limitations. The bryozoan fossilization process often involves fragmentation (Key et al. 2016), so finding complete colonies may be a challenge. If the zoecial cavities are filled with carbonate cements and/or matrix of similar density to the zoecial walls, X-ray images may not show the brightness contrast necessary to see the more subtle growth checks (Wyse Jackson and Buttler 2015). If the bryozoan skeletal carbonate has been diagenetically altered, the isotope values may be altered as well (Key et al. 2005b).

## CONCLUSIONS

The present study shows that growth checks in a temperate bryozoan are annual and occur during the cold temperatures of the austral winter. X-ray characterization of checks provided the highest resolution and was the easiest, but somewhat subjective, method for counting growth segments. Branch width variation is more objective, but can be confounded by branch swelling from ovicell growth. The isotope method is the most expensive, most time-consuming, and least spatially-resolved method, but the only method that directly correlates the growth segments with seasonal temperature cycles. Our study shows that stable isotopes can be successfully analyzed in unbleached bryozoans with the organic components intact. In *M. chathamensis* from New Zealand, the results of these three different methods of determining growth were mostly consonant.

The annual growth cycle in this species is dominated by temperature change, but may also include a higher-frequency algal bloom signal. A winter growth check of high skeletal density gives way to rapid growth with a wider branch and less-dense carbonate in spring and early summer. Maximum branch width occurs when ovicells appear in late summer/early autumn, prior to constriction as winter arrives again. A larger sample size is needed to statistically discriminate between the relative effects of environmental, astogenetic, and colony factors on growth in this species.

This species precipitates its skeleton in isotopic equilibrium with its surrounding water. The  $\delta^{18}\text{O}$ -derived temperatures documented inter-annual variations, which may be related to fluctuations in the position of the SF across the Snares Platform. The temperatures measured in the largest and most densely-sampled colony were broadly correlated with inter-annual variations related to the SOI.

## ACKNOWLEDGMENTS

We thank: the skipper and crew of the RV POLARIS II (University of Otago, New Zealand) for help with field work, D Campbell (University of Otago, New Zealand) for X-ray imaging, C DeWet and S Sylvester (Franklin and Marshall College) for micromilling, S Timsic and D Besic (University of Saskatchewan, Canada) for isotope analyses, and H Neil (National Institute of Water and Atmospheric Research, New Zealand) for oceanographic data retrieval. Funding was provided by the Dickinson College Research and Development Committee and a NASA Cool Climate Grant from the Dickinson College Center for Sustainability Education. This manuscript was greatly improved by the comments of A O’Dea (Smithsonian Tropical Research Institute, Panama) and three anonymous reviewers.

## LITERATURE CITED

- Ashcroft L, Gergis J, Karoly DJ. 2016. Long-term stationarity of El Niño–Southern Oscillation teleconnections in southeastern Australia. *Clim Dyn.* 46:2991–3006. <https://doi.org/10.1007/s00382-015-2746-3>
- Bader B. 2000. Life cycle, growth rate and carbonate production of *Cellaria sinuosa*. In: Herrera Cubilla A, Jackson JBC, editors. Proceedings of the 11th International Bryozoology Association conference. Balboa, Republic of Panama: Smithsonian Tropical Research Institute. p. 136–144.
- Bader B, Schäfer P. 2004. Skeletal morphogenesis and growth check lines in the Antarctic bryozoan *Melicerita obliqua*. *J Nat Hist.* 38:2901–2922. <https://doi.org/10.1080/00222930310001657685>
- Bader B, Schäfer P. 2005. Impact of environmental seasonality on stable isotope composition of skeletons of the temperate bryozoan *Cellaria sinuosa*. *Palaeogeogr Palaeoclimatol Palaeoecol.* 226(1–2):58–71. <https://doi.org/10.1016/j.palaeo.2005.05.007>
- Belkin IM, Cornillon PC. 2003. SST fronts of the Pacific coastal and marginal seas. *Pac Oceanogr.* 1(2):90–113.
- Brey T, Gerdes D, Gutt J, Mackensen A, Starmans A. 1999. Growth and age of the Antarctic bryozoan *Cellaria incula* on the Weddell Sea shelf. *Antarct Sci.* 11(4):408–414. <https://doi.org/10.1017/S0954102099000516>
- Brey T, Gutt J, Mackensen A, Starmans A. 1998. Growth and productivity of the high Antarctic bryozoan *Melicerita obliqua*. *Mar Biol.* 132(2):327–333. <https://doi.org/10.1007/s002270050398>
- Butler ECV, Butt JA, Lindstrom EJ, Tildesley PC. 1992. Oceanography of the Subtropical Convergence Zone around southern New Zealand. *N Z J Mar Freshw Res.* 26(2):131–154. <https://doi.org/10.1080/00288330.1992.9516509>
- Campanelli A, Massolo S, Grilli F, Marini M, Paschini E, Rivaro P, Artegiani A, Jacobs SS. 2011. Variability of nutrient and thermal structure in surface waters between New Zealand and Antarctica, October 2004–January 2005. *Polar Res.* 30:7064. <https://doi.org/10.3402/polar.v30i0.7064>
- Chiswell SM. 1996. Variability in the Southland Current, New Zealand. *N Z J Mar Freshw Res.* 30(1):1–17. <https://doi.org/10.1080/00288330.1996.9516693>
- Cocito S, Novosel M, Novosel A. 2004. Carbonate bioformations around underwater freshwater springs in the north-eastern Adriatic Sea. *Facies.* 50:13–17. <https://doi.org/10.1007/s10347-004-0007-8>
- Craig H. 1957. Isotopic standards for carbon and oxygen and correction factors for mass spectrometric analysis of carbon dioxide. *Geochim Cosmochim Acta.* 12(1–2):133–149. [https://doi.org/10.1016/0016-7037\(57\)90024-8](https://doi.org/10.1016/0016-7037(57)90024-8)
- Crowley SE, Taylor PD. 2000. Stable isotope composition of modern bryozoan skeletal carbonate from the Otago Shelf, New Zealand. *N Z J Mar Freshw Res.* 34(2):331–351. <https://doi.org/10.1080/00288330.2000.9516936>

- Erez J. 1978. Vital effect on stable-isotope composition seen in foraminifera and coral skeletons. *Nature*. 273:199–202. <https://doi.org/10.1038/273199a0>
- Forester RM, Sandberg PA, Anderson TF. 1973. Isotopic variability of cheilostome bryozoan skeletons. *In: Larwood GP, editor. Living and Fossil Bryozoa*. New York: Academic Press. p. 79–94.
- Friedman I, O'Neil J, Cebula G. 1982. Two new carbonate stable isotope standards. *Geostand Newsl*. 6(1):11–12. <https://doi.org/10.1111/j.1751-908X.1982.tb00340.x>
- Garner DM. 1969. The seasonal range of sea temperature on the New Zealand Shelf. *N Z J Mar Freshw Res*. 3(2):201–208. <https://doi.org/10.1080/00288330.1969.9515289>
- Gordon DP, Mawatari SF. 1992. Atlas of marine-fouling Bryozoa of New Zealand ports and harbours. *Misc Pubs NZ Oceanogr Inst*. 107:1–52.
- Hageman SJ, Bayer MM, Todd CD. 1999. Partitioning phenotypic variation: genotypic, environmental and residual components from bryozoan skeletal morphology. *J Nat Hist*. 33: 1713–1735. <https://doi.org/10.1080/002229399299815>
- Heath RA. 1985. A review of the physical oceanography of the seas around New Zealand - 1982. *N Z J Mar Freshw Res*. 19(1):79–124. <https://doi.org/10.1080/00288330.1985.9516077>
- Hopkins J, Shaw AGP, Challenor P. 2010. The Southland Front, New Zealand: variability and ENSO correlations. *Cont Shelf Res*. 30(14):1535–1548. <https://doi.org/10.1016/j.csr.2010.05.016>
- Jillett J. 1969. Seasonal hydrology of waters off the Otago Peninsula south-eastern, New Zealand. *N Z J Mar Freshw Res*. 3(3):349–375. <https://doi.org/10.1080/00288330.1969.9515303>
- Jimenez-Lopez C, Romanek CS, Caballero E. 2006. Carbon isotope fractionation in synthetic magnesian calcite. *Geochim Cosmochim Acta*. 70(5):1163–1171. <https://doi.org/10.1016/j.gca.2005.11.005>
- Keith ML, Weber JN. 1965. Systematic relationships between carbon and oxygen isotopes in carbonates deposited by modern corals and algae. *Science*. 150(3695):498–501. <https://doi.org/10.1126/science.150.3695.498>
- Key MM Jr, Hollenbeck PM, O'Dea A, Patterson WP. 2013b. Stable isotope profiling in modern marine bryozoan colonies across the Isthmus of Panama. *Bull Mar Sci*. 89(4):837–856. <http://dx.doi.org/10.5343/bms.2012.1056>
- Key MM Jr, Wyse Jackson PN, Håkansson E, Patterson WP, Moore MD. 2005a. Gigantism in Permian trepostomes from Greenland: testing the algal symbiosis hypothesis using  $\delta^{13}\text{C}$  and  $\delta^{18}\text{O}$  values. *In: Moyano G HI, Cancino JM, Wyse Jackson PN, editors. Bryozoan Studies 2004*. Leiden: Balkema Publishers. p. 141–151.
- Key MM Jr, Wyse Jackson PN, Patterson WP, Moore MD. 2005b. Stable isotope evidence for diagenesis of the Ordovician Courtown and Tramore Limestones, south-eastern Ireland. *Isr J Earth Sci*. 23(1):25–38. <http://dx.doi.org/10.3318/IJES.2005.23.1.25>
- Key MM Jr, Zágoršek K, Patterson WP. 2013a. Paleoenvironmental reconstruction of the Early to Middle Miocene Central Paratethys using stable isotopes from bryozoan skeletons. *Int J Earth Sci*. 102(1):305–318. <https://doi.org/10.1007/s00531-012-0786-z>
- Key MM Jr, Wyse Jackson PN, Felton SH. 2016. Intracolony variation in colony morphology in reassembled fossil ramose stenolaemate bryozoans from the Upper Ordovician (Katian) of the Cincinnati Arch region, USA. *J Paleontol*. 90(3):400–412. <https://doi.org/10.1017/jpa.2016.66>
- Kim S-T, Mucci A, Taylor BE. 2007. Phosphoric acid fractionation factors for calcite and aragonite between 25 and 75°C: Revisited. *Chem Geol*. 246(3–4):135–146. <https://doi.org/10.1016/j.chemgeo.2007.08.005>
- Kim S-T, O'Neil JR. 1997. Equilibrium and nonequilibrium oxygen isotope effects in synthetic carbonates. *Geochim Cosmochim Acta*. 61(16):3461–3475. [https://doi.org/10.1016/S0016-7037\(97\)00169-5](https://doi.org/10.1016/S0016-7037(97)00169-5)

- Knowles T, Taylor PD, Williams M, Haywood AM, Okamura B. 2009. Pliocene seasonality across the North Atlantic inferred from cheilostome bryozoans. *Palaeogeogr Palaeoclimatol Palaeoecol.* 277(3–4):226–235. <https://doi.org/10.1016/j.palaeo.2009.04.006>
- Knowles T, Leng MJ, Williams M, Taylor PD, Sloane HJ, Okamura B. 2010. Interpreting seawater temperature range using oxygen isotopes and zooid size variation in *Pentapora foliacea* (Bryozoa). *Mar Biol.* 157(6):1171–1180. <https://doi.org/10.1007/s00227-010-1397-5>
- Lombardi C, Cocito S, Occhipinti-Ambrogi A, Hiscock K. 2006. The influence of seawater temperature on zooid size and growth rate in *Pentapora fascialis* (Bryozoa: Cheilostomata). *Mar Biol.* 149:1103–1109. <https://doi.org/10.1007/s00227-006-0295-3>
- Lombardi C, Cocito S, Hiscock K, Occhipinti-Ambrogi A, Setti M, Taylor PD. 2008. Influence of seawater temperature on growth bands, mineralogy and carbonate production in a bio-constructive bryozoan. *Facies.* 54:333–342. <https://doi.org/10.1007/s10347-008-0143-7>
- Lombardi C, Taylor PD, Cocito S. 2010. Systematics of the Miocene-Recent bryozoan genus *Pentapora* (Cheilostomata). *Zool J Linn Soc.* 160:17–39. <https://doi.org/10.1111/j.1096-3642.2009.00594.x>
- McClelland HLO, Taylor PD, O’Dea A, Okamura B. 2014. Revising and refining the bryozoan *zs*-MART seasonality proxy. *Palaeogeogr Palaeoclimatol Palaeoecol.* 410:412–420. <https://doi.org/10.1016/j.palaeo.2014.06.011>
- Murphy RJ, Pinkerton MH, Richardson KM, Bradford-Grieve J, Boyd PW. 2001. Phytoplankton distributions around New Zealand derived from SeaWiFS remotely-sensed ocean colour data. *N Z J Mar Freshw Res.* 35(2):343–362. <https://doi.org/10.1080/00288330.2001.9517005>
- O’Dea A. 2003. Seasonality and variation in zooid size in Panamanian encrusting bryozoans. *J Mar Biol Assoc U K.* 83:1107–1108. <https://doi.org/10.1017/S0025315403008348h>
- O’Dea A. 2005. Zooid size parallels contemporaneous oxygen isotopes in a large colony of *Pentapora foliacea* (Bryozoa). *Mar Biol.* 146(6):1075–1081. <https://doi.org/10.1007/s00227-004-1523-3>
- O’Dea A, Jackson JBC. 2002. Bryozoan growth mirrors contrasting seasonal regimes across the Isthmus of Panama. *Palaeogeogr Palaeoclimatol Palaeoecol.* 185(1–2):77–94. [https://doi.org/10.1016/S0031-0182\(02\)00278-X](https://doi.org/10.1016/S0031-0182(02)00278-X)
- O’Dea A, Okamura B. 1999. Influence of seasonal variation in temperature, salinity and food availability on module size and colony growth of the estuarine bryozoan *Conopeum seurati*. *Mar Biol.* 135(4):581–588. <https://doi.org/10.1007/s002270050659>
- O’Dea A, Okamura B. 2000. Intracolony variation in zooid size in cheilostome bryozoans as a new technique for investigating palaeoseasonality. *Palaeogeogr Palaeoclimatol Palaeoecol.* 162(3–4):319–332. [http://dx.doi.org/10.1016/S0031-0182\(00\)00136-X](http://dx.doi.org/10.1016/S0031-0182(00)00136-X)
- Pätzold J, Ristedt H, Wefer G. 1987. Rate of growth and longevity of a large colony of *Pentapora foliacea* (Bryozoa) recorded in their oxygen isotope profiles. *Mar Biol.* 96(4):535–538. <https://doi.org/10.1007/BF00397971>
- Patterson WP. 2017. *Environmental Stable Isotope Chemistry*. Kendall Hunt, Dubuque, IA.
- Rahmstorf S. 1992. Modelling ocean temperatures and mixed-layer depths in the Tasman Sea off the South Island, New Zealand. *N Z J Mar Freshw Res.* 26(1):37–51. <https://doi.org/10.1080/00288330.1992.9516498>
- Reid C. 2014. Growth and calcification rates in polar bryozoans from the Permian of Tasmania, Australia. *Studi Trent Sci Nat.* 94:189–197.
- Ridgway NM. 1969. Temperature and salinity of sea water at the ocean floor in the New Zealand region. *N Z J Mar Freshw Res.* 3(1):57–72. <https://doi.org/10.1080/00288330.1969.9515278>
- Rintoul SR, Donguy JR, Roemmich DH. 1997. Seasonal evolution of upper ocean thermal structure between Tasmania and Antarctica. *Deep Sea Res Part I Oceanogr Res Pap.* 44(7):1185–1202. [https://doi.org/10.1016/S0967-0637\(96\)00125-2](https://doi.org/10.1016/S0967-0637(96)00125-2)
- Romanek CS, Grossman EL. 1989. Stable isotope profiles of *Tridacna maxima* as environmental indicators. *Palaios.* 4(5):402–413. <https://doi.org/10.2307/3514585>

- Shaw AGP, Vennell R. 2001. Measurements of an oceanic front using a front following algorithm for AVHRR SST imagery. *Remote Sens Environ.* 75(1):47–62. [https://doi.org/10.1016/S0034-4257\(00\)00155-3](https://doi.org/10.1016/S0034-4257(00)00155-3)
- Sikes EL, Howard WR, Neil HL, Volkman JK. 2002. Glacial-interglacial sea surface temperature changes across the subtropical front east of New Zealand based on alkenone unsaturation ratios and foraminiferal assemblages. *Paleoceanography.* 17(2):1–13. <https://doi.org/10.1029/2001PA000640>
- Smith AM. 2007. Age, growth and carbonate production by erect rigid bryozoans in Antarctica. *Palaeogeogr Palaeoclimatol Palaeoecol.* 256(1–2):86–98. <https://doi.org/10.1016/j.palaeo.2007.09.007>
- Smith AM. 2014. Growth and calcification of marine bryozoans in a changing ocean. *Biol Bull.* 226(3):203–210. <https://doi.org/10.1086/BBLv226n3p203>
- Smith AM, Key MM Jr. 2004. Controls, variation and a record of climate change in a detailed stable isotope profile from a single bryozoan skeleton. *Quat Res.* 61(2):123–133. <https://doi.org/10.1016/j.yqres.2003.11.001>
- Smith AM, Lawton EI. 2010. Growing up in the temperate zone: age, growth, calcification and carbonate mineralogy of *Melicerita chathamensis* (Bryozoa) in southern New Zealand. *Palaeogeogr Palaeoclimatol Palaeoecol.* 298(3–4):271–277. <https://doi.org/10.1016/j.palaeo.2010.09.033>
- Smith RO, Vennell R, Bostock HC, Williams MJM. 2013. Interaction of the subtropical front with topography around southern New Zealand. *Deep Sea Res Part I Oceanogr Res Pap.* 76:13–26. <https://doi.org/10.1016/j.dsr.2013.02.007>
- Stebbing ARD. 1971. Growth of *Flustra foliacea* (Bryozoa). *Mar Biol.* 9(3):267–273. <https://doi.org/10.1007/BF00351389>
- Tarutani T, Clayton RN, Mayeda TK. 1969. The effects of polymorphism and magnesium substitution on oxygen isotope fractionation between calcium carbonate and water. *Geochim Cosmochim Acta.* 33(8):987–996. [https://doi.org/10.1016/0016-7037\(69\)90108-2](https://doi.org/10.1016/0016-7037(69)90108-2)
- Tilburg CE, Hurlburt HE, O'Brien JJ, Shriver JF. 2002. Remote topographic forcing of a baroclinic western boundary current: an explanation for the Southland Current and the pathway of the subtropical front east of New Zealand. *J Phys Oceanogr.* 32:3216–3232. [https://doi.org/10.1175/1520-0485\(2002\)032<3216:RTFOAB>2.0.CO;2](https://doi.org/10.1175/1520-0485(2002)032<3216:RTFOAB>2.0.CO;2)
- Uttley GH, Bullivant JS. 1972. Biological results of the Chatham Islands 1954 Expedition. Part 7. Bryozoa Cheilostomata. *Mem NZ Oceanograph Inst.* 57:1–61.
- van Hardenbroek M, Leuenerberger M, Hartikainen H, Okamura B, Heiri O. 2016. Stable carbon and hydrogen isotopes in freshwater bryozoans and their statoblasts – experimental and field data. *Hydrobiologia.* 765:209–223. <https://doi.org/10.1007/s10750-015-2414-y>
- Wurster CM, Patterson WP, Cheatham MM. 1999. Advances in micromilling techniques: a new apparatus for acquiring high-resolution oxygen and carbon stable isotope values and major/minor elemental ratios from accretionary carbonate. *Comput Geosci.* 25(10):1159–1166. [https://doi.org/10.1016/S0098-3004\(99\)00052-7](https://doi.org/10.1016/S0098-3004(99)00052-7)
- Wyse Jackson PN, Buttler CJ. 2015. Part G, Vol. 2, Ch. 3: Preparation, imaging, and conservation of Paleozoic bryozoans for study. *Treat Invert Paleontol Online.* 63:1–15. <http://dx.doi.org/10.17161/to.v0i0.4854>

